ELSEVIER

Polymer 43 (2002) 4699–4708

polymer

www.elsevier.com/locate/polymer

Time resolved study of shear-induced crystallization of poly(*p*-dioxanone) polymers under low-shear, nucleation-enhancing shear conditions by small angle light scattering and optical microscopy

Ferass M. Abuzaina[1], Benjamin D. Fitz*, Saša Andjelić, Dennis D. Jamiolkowski

Department of Polymer and Suture Technologies, Ethicon, a Johnson & Johnson Company, P.O. Box 151, Somerville, NJ 08876-0151, USA

Received 4 December 2001; received in revised form 22 April 2002; accepted 24 April 2002

Abstract

Isothermal crystallization of the biodegradable homopolymer polyester poly(*p*-dioxanone) (PDS), and the *p*-dioxanone copolymer with glycolide PDS-copolymer were studied in situ and in real-time under quiescent or nucleation-enhancing shear conditions. It was found that the spherulitic growth rates remain unchanged with shear, while the nucleation density increases dramatically. Nucleation-enhancing shear conditions, which do not alter the general spherulitic morphology, consist of a short-duration step-shear. This is in contrast to isothermal crystallization under steady-shear conditions, where at low-shear rates, fibrillar crystalline structures form. At high crystallization temperatures, where under quiescent conditions crystal development requires several days, both PDS, and the PDS-copolymer can be made to crystallize in several hours by the imposition of a step-shear.

Keywords: Poly(*p*-dioxanone); Nucleation-enhancing shear; Deforming shear

1. Introduction

The development of crystallinity during industrial polymer processing is vastly complex, involving diverse temperature and mechanical stress gradients. Examining one parameter at a time simplifies the problem. To that end, in this paper we discuss the effect of shear on isothermal crystallization. Under carefully controlled mechanical perturbations two shear regimes can be recognized. The first set of mild conditions of applied shear, hereafter referred to as *nucleation-enhancing* shear fields, is the situation where no changes in crystal morphology, crystal form, or lamellar spacing are introduced. The second regime, under more harsh shear conditions, hereafter referred to as *deforming* shear, undesirably increases the complexity of the problem by inducing a variety of morphological changes. These problems include reorientation of formed crystallites [1–3], formation of oriented crystallites [3,4] (fibrillar, or row-nucleated morphologies), changes in crystal form [5,6], surface crystallization [4], shear-induced degradation, and problematic temperature fluctuations in the sample via dissipative heating [7]. To restate: nucleation-enhancing shear conditions are those sufficiently intense so as to enhance crystallization kinetics, but not so severe as to influence the resulting crystalline morphology (other than, perhaps, spherulite size, discussed later).

It has been shown that nucleation rates exponentially increase with crystallization time under steady-shear, while growth rates are either unaffected [8], or only slightly increased [9]. Shear-enhanced nucleation is explained in the following way. Chains under strain are perturbed from the random coil configuration, with two consequences: (1) the system entropy is reduced, effectively increasing the degree of undercooling [10] and the polymer's melting temperature, and (2) the induced chain extension provides a higher probability for favorable chain conformation for registry with heterogeneous nuclei, secondary nuclei, and with other extended chains allowing a significant degree of homogeneous nucleation to occur. Additionally, small crystal aggregates may form from deformed or broken spherulites which may act as additional self-heterogeneous nuclei [11].

It was pointed out by Keller and Kolnaar [12] that the effects of shear rate and total strain should be examined

* Corresponding author. Tel.: +1-908-218-2828; fax: +1-908-218-2840.
E-mail address: bfitz@ethus.jnj.com (B.D. Fitz).
[1] Present address: Department of Chemical Engineering, Chemistry and Material Science, Polytechnic University, Six Metrotech Center, Brooklyn, NY 11201, USA.

0032-3861/01/$ - see front matter
PII: S0032-3861(02)00300-2

independently. One approach to studying these factors was examined by a few authors by applying a step-shear [3,4,9,13,14]. However, these studies reported morphological changes indicative of a deforming shear regime.

The objective of the present work is to examine the influence of nucleation-enhancing shear conditions on polymer crystallization. We will establish the conditions for nucleation-enhancing shear for the biodegradable polyester and polyester copolymer under investigation. We will investigate the effect of nucleation-enhancing shear on nucleation and growth rates. And we will examine the effects of nucleation-enhancing shear on the over-all crystallization kinetics. For experimental convenience, the studies will take advantage of previous work [15,16] finding a polymer capable of crystallizing over a wide temperature range with slow crystallization kinetics and low nucleation densities. Finally, we will examine the effects of molecular structure by comparing the results with a related copolymer. As the dynamic changes in structure are required at early stages of the process, and over short time intervals, and it is of interest to follow the development of order across a wide range of length-scales in real-time, we have constructed a small angle light scattering instrument that is described briefly in Section 2.

2. Experimental section

2.1. Materials

The two polymers used in this study were the following. The first was poly(*p*-dioxanone) homopolymer [17,18] (hereafter, referred to as PDS), having an inherent viscosity (IV) of 1.76 dl/g in hexaflouroisopropanol (HFIP) at 25 °C at a concentration of 0.1 g/dl. The PDS weight average molecular weight, M_w, was 82,000 g/mol, with a number average molecular weight, M_n, of 38,000 g/mol (by GPC). The glass transition temperature, T_g, of PDS was −12 °C; the equilibrium melting point, T_m^0, was approximately 140 °C. The second polymer was an 89/11 (w/w%) *p*-dioxanone/glycolide segmented block copolymer (hereafter, referred to as PDS-copolymer), having an IV of 1.75 dl/g; M_w 77,000 g/mol, M_n 27,000 g/mol; T_g −10 °C, and a T_m^0 of approximately 140 °C. The polymers were prepared at Ethicon by a tin catalyzed ring-opening bulk polymerization. These polymers contained a dye (medical devices made from these polymers are dyed to aid in their visualization at the surgical site) which was D&C Violet No.2 at approximately 0.2 wt%. It has previously been determined that this small amount of dye has no affect on crystallization phenomena in these polymers [19]. Because of the high sensitivity of these polyesters to hydrolytic degradation, the samples were stored under high vacuum; during testing, exposure to ambient atmosphere was limited. Selected samples were examined for molecular weight and IV reduction following the experimental procedure, and no significant reductions were found (<2%).

2.2. Small angle light scattering

A 20 mW He–Ne laser (Uniphase, Manteca, CA) with $\lambda = 0.633$ μm was used as the light source. The light was directed through an uncoated right-angle glass prism, followed by the compensator (quartz quarter-wave retardation plate) and the first polarizer. The laser beam then reached the sample, which was enclosed in the optical Linkam CSS 450 Cambridge Shearing System supplied with a precise temperature control unit. The light emerging from the sample passed through a broadband beam sampler (splitter), where approximately 5% of the light was redirected and focused into a silicon photodiode. This photo-detector was used to measure the changes in transmitted laser intensity as a function of time. By recording the voltage displayed by an amplifier connected to the detector output, the transmission, I/I_0, was measured. A relative extent of crystallinity may be derived from relative changes in transmission as crystallization proceeds. The major portion of the light beam, unaffected by the sampler, advanced to the analyzer. From there, the h_v (incident light polarized vertically and scattered light polarized horizontally) scattering pattern was projected onto a high quality paper screen using a 50 mm dielectric mirror.

Coordinates in the projection plane were determined by two angles, θ and μ. The scattering vector was calibrated using the four concentric circles method as described elsewhere [20]. The scattering profiles were recorded by a NEC TI324A CCD industrial high-resolution monochrome camera, equipped with a Nikon 28 mm lens and positioned on the optical rails. The images were captured and analyzed using Image Pro Plus® (version 4.0) software. The entire setup was mounted on a research grade optical table supported by vibrational isolators.

2.3. Hot stage optical microscopy

Optical microscopy was performed with a Nikon SHZ-U optical microscope in conjunction with a Micron i308 low light integrating camera; all observations were viewed through crossed polars. The sample was held in the Linkam shear stage, providing precise temperature and shear control, as described later. All images presented here were captured at a 6× magnification, and a scale bar is shown in the microscopy figures. For enhancement in appearance for publication, all optical microscopy images have been contrast-inverted; dark fields are light and vice versa. Additional details may be found in Ref. [16].

2.4. Shear cell

For both hot stage optical microscopy and SALS, a

parallel-plate shear apparatus (Linkam CSS 450. Linkam Scientific Instruments, Ltd, Tadworth, Surrey, UK) was used to host a sample while precisely controlling the sample temperature and thickness. The cell was designed to apply a variety of shear modes—step, steady or oscillatory, at a wide range of shear rates and over-all strains. The circular aperture in the parallel windows for viewing with an optical microscope or passing the SALS laser was located 7.5 mm from the center of the windows, and had a diameter of 2.8 mm. A concern exists about achieving a desired deformation of the polymer sample, since torsional shear of polymer melts under high deformations is known to be problematic. To address this, we have confirmed by visual inspection of samples after each crystallization experiment (the samples remain intact during the removal process from the shear cell; as the polymer is adhering to both upper and lower shear cell windows, care must be exercised to avoid shattering the windows), that for the step-shear rates used here, no melt fracture, melt slip, sample expulsion or the like occurred.

2.5. Experimental procedure

Prior to use, the samples were stored under nitrogen. All samples were melted at 140 °C for 10 min to erase any thermal or mechanical history. After 5 min at 140 °C, when the sample was entirely molten, the upper lid of the shear cell was lowered to achieve our desired sample-thickness of about 140 μm (verified after each experiment). Following the melting step the samples were quenched to the desired crystallization temperature, and then either allowed to quiescently crystallize or the desired shear mode was applied. Two shear modes were used: a step-shear at a given shear rate for a given strain and resulting strain-duration (Section 3), or continuously sheared at a given shear rate for the entire crystallization process. The desired shear was applied at the moment the sample reached the crystallization temperature. Selected samples were examined for molecular weight and IV reduction following each experiment, and no significant reductions were found ($<2\%$).

3. Results and discussion

In this section we present our results on the enhancement of crystallization by the application of nucleation-enhancing shear. First, we examine the effects of steady-shear on the crystallization kinetics and morphology. Then we present results from an application of a step-shear. Finally, we show that the application of a nucleation-enhancing step-shear is sufficient to allow nucleation of the crystallization process followed by growth under thermal conditions where quiescent crystallization does not normally occur.

Our objective is to study the influence of shear on the crystallization behavior of the biodegradable polyesters, PDS and the PDS-copolymer under nucleation-enhancing shear conditions. That is, shear conditions that were sufficiently intense as to enhance the crystallization kinetics, but not so severe as to influence the resulting morphology. We should note that these studies would examine structure and morphological changes on only the micron-scale and not the crystalline lamellar level. By performing our studies in the nucleation-enhancing shear regime we can hope to better understand the nature of the well-known crystallization enhancement by shear.[2] A first step in probing the limits of deforming to nucleation-enhancing shear regimes consisted of examining the crystallization of these polymers under steady-shear conditions.

3.1. Steady-shear crystallization

It was of interest to determine the limits of nucleation-enhancing shear conditions on the polymers under study. At some point in the crystallization process the polymer is ‘crosslinked’ by crystallites and forms a physical gel [3,21]. On reaching or nearing this gel condition, a nucleation-enhancing shear regime will become deforming as the increasing entanglements via crystallite ‘crosslinking’ will serve to allow the elongated polymer chains to pull apart spherulitic structures attached at either end. The nucleation-enhancing to deforming shear regime crossover will be a function of strain, shear rate, and temperature for a given polymer. In addition to the enhancement of chain entanglements by crystallite crosslinking, we have observed by microscopy the following spherulite–spherulite interactions during shear. For a typical sample, the parallel window separation was approximately 140 μm. At a point in time during the steady-shear crystallization process, spherulites of dimensions on the order of half the window gap will begin to collide. This is because polymer chains in the melt adhere to the walls of both the stationary plate and the moving plate—the moving boundary is between the windows. This is clearly observable via optical microscopy. Under the microscope one observes stationary spherulites (evidently tethered by adhering polymer chains to the stationary window), while near the moving window, spherulites (evidently tethered to that window) are observed to translate across the microscope field of view. During the early stages of crystallization, one observes a set of developing stationary spherulites with another set of moving spherulites passing over them. However, when the spherulites are sufficiently large they collide resulting in significant spherulite deformation, resulting in fibrillar morphologies. An example of the growth-to-collision sequence is shown in Fig. 1.

The effect of continuous steady-shear (shear rate of 0.1 s^{-1}) was examined on both PDS and the PDS-copolymer. It was found that even this low-shear rate induces non-spherulitic, deformed-spherulitic, and fibrillar-like morphological

[2] The literature on shear-enhanced crystallization kinetics has been nicely summarized in Refs. [9,14].

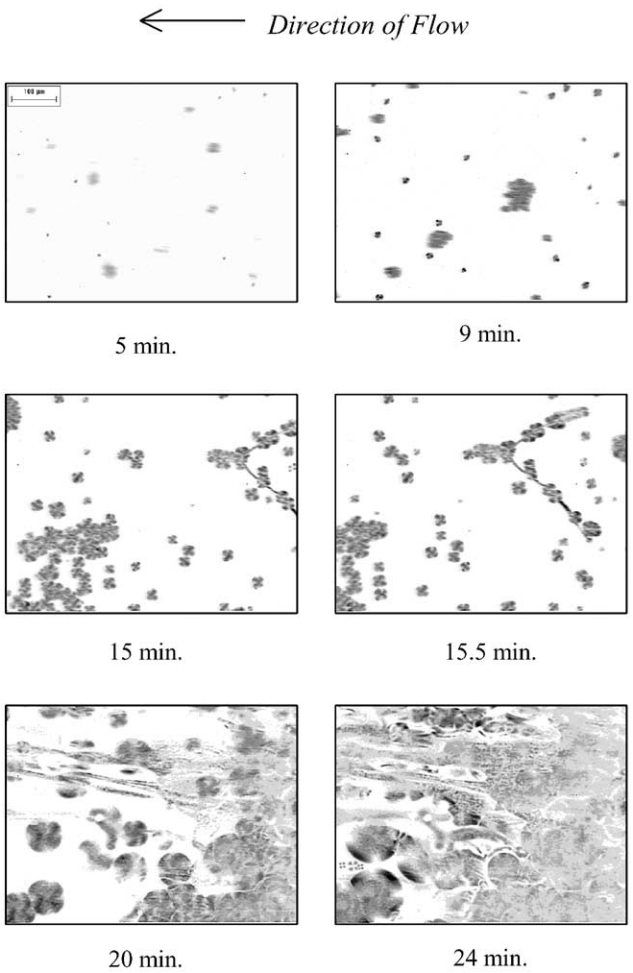

Fig. 1. Deformation of PDS spherulites observed via optical microscopy at selected times during steady-shear (shear rate of 0.1 s^{-1}) at 80 °C. The direction of flow is indicated. The sample-thickness was 140 μm.

features early in the course of crystallization. Such features are directly observed by optical microscopy and also by their characteristic streak scattering patterns [22] in SALS, as shown in Fig. 2. The example shown in this figure was a PDS sample crystallized under the above steady-shear at 80 °C for 24 min. This phenomenon is present for both PDS and the PDS-copolymer under these steady-shear conditions. In spite of the deforming shear conditions, the relative extent of crystallization time-course data could be collected in the early stages of the process, before film damage occurred. The data were obtained by a decay in the SALS transmission intensity, and were found to be well-fit by an Avrami model. The Avrami parameters are: $n = 6.1$, $t_{1/2} = 2.6$, $k = 6.5 \times 10^{-10}$. The Avrami exponent, n, of 6.1, shows that the imposition of steady-shear greatly accelerates the crystallization process. This high n value is in accord with those found previously during steady-shear crystallization for poly(ethylene oxide) [7] where a maximum n value of 6.7 (sheared at 44.6 s^{-1}) was observed, and poly(caprolactone) where values of n of 5.5 (sheared at

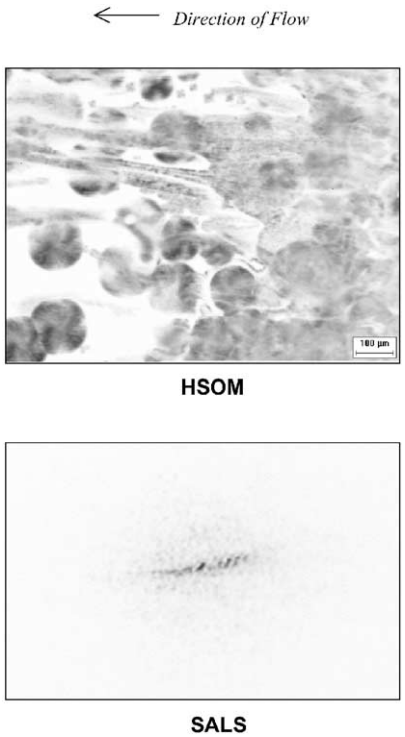

Fig. 2. Optical micrograph and SALS image obtained on deformed PDS spherulites. The sample was exposed to steady-shear (shear rate of 0.1 s^{-1}) at 80 °C for 24 min. The direction of flow is indicated. The sample-thickness was 140 μm.

26.9 s^{-1}) [7] and 8 (at a shear stress of 1800 Pa) [23] were observed.

3.2. Step-shear crystallization

Our next approach involved looking at crystallization under less aggressive shear force-fields, where the shear was applied for a short, 1 s duration, at desired shear rates. It is shown in Fig. 3a and b via optical microscopy and depolarized light scattering images that a shear rate of 60 s^{-1} applied for 1 s does not disturb the morphological development in either polymer. Spherulites develop and grow in an undisturbed fashion at random locations throughout the sample. This figure shows that for these shear conditions, the sole effect is an increase in nucleation density. This is directly revealed by the optical microscope images, and indirectly by the increased intensity in the light scattering patterns. Having identified a mild shear regime for these polymers, we investigated next the influence of step-shear on the over-all crystallization kinetics.

We utilize the change in SALS light transmission through our samples as a measure of the development of crystallinity. The laser light transmission decays as the sample fills with crystalline structure (density and anisotropy fluctuations increase) and the turbidity increases. The changes in relative extent of crystallinity obtained from this measurement for PDS during quiescent crystallization over a wide range of crystallization temperatures is shown in

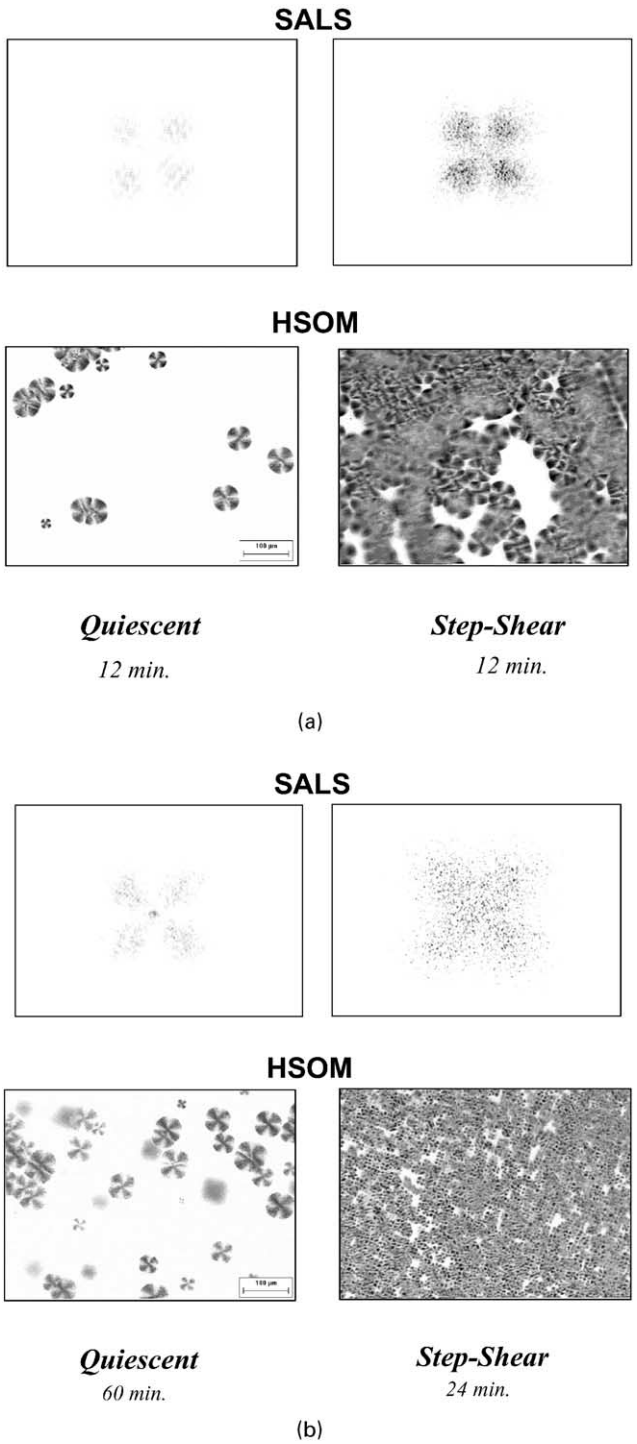

Fig. 3. SALS images and optical micrographs contrasting nucleation density and distribution of spherulite sizes for: (a) PDS crystallized isothermally at 75 °C for 12 min under quiescent and step-shear (60 s^{-1} for 1 s) conditions, and (b) PDS-copolymer compared under the same conditions as (a) except at 70 °C.

Fig. 4. The decrease in crystallization kinetics with increasing crystallization temperature is apparent. The solid curves in the figure are best-fits to the Avrami function [24], $-\ln(1-x) = kt^n$, where x is the relative extent of crystallization, k is a composite rate constant, and n is the

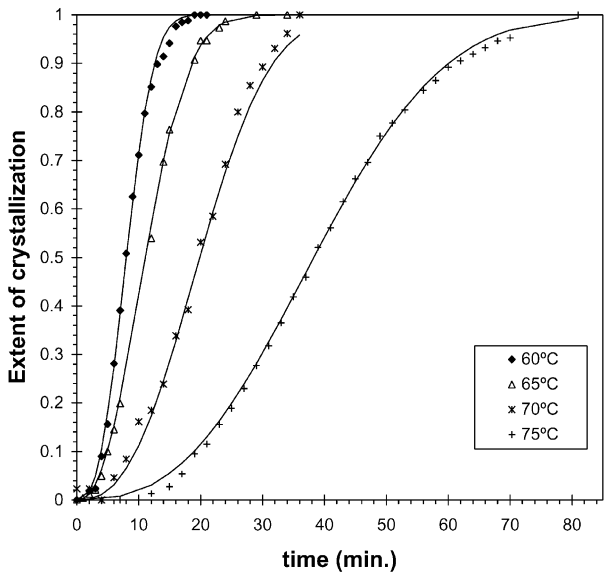

Fig. 4. Extent of quiescent crystallization time-course measured by SALS transmission at selected crystallization temperatures for PDS.

Avrami exponent. These parameters are related to the crystallization half-time, $t_{1/2}$, by $t_{1/2} = [\ln(2)/k]^{1/n}$. We emphasize that $t_{1/2}$ is the time required to achieve 50% of the ultimate degree of crystallinity (approx. 40% for PDS), not the time required to achieve an actual volume fraction of 50% crystallinity. The Avrami parameters obtained by this method are given in Table 1.

The quiescent crystallization kinetics characterized by the Avrami model parameters n and $t_{1/2}$ of PDS over a wide range of crystallization temperatures have been determined by this SALS transmission measurement yielding an average Avrami n of 2.5. The crystallization half-time values, $t_{1/2}$, are in agreement with those determined previously (the $t_{1/2}$ comparison is shown in Fig. 5, and the n comparison is shown in Fig. 6) obtained using an experimental technique measuring the decrease in dipolar mobility during crystallization, dielectric relaxation spectroscopy (DRS) [15]. The Avrami n value is also in agreement with n values obtained from calorimetry [19] and SAXS [25]. The Avrami n data in Table 1 also indicate that the n parameter is essentially independent of temperature, indicating that the crystalline morphological development occurs in the same manner, but at kinetically governed temperature-dependent rates. A variation in n with changing crystallization conditions would indicate a change in the method of morphological development [24]. These findings agree with our optical microscopy observations.

The influence of a small duration, 1 s shear, at a shear rate of 60 s^{-1} on the progress of crystallization is dramatic, as shown in Fig. 7a for PDS and Fig. 7b for the PDS-copolymer. Here the extent of crystallization time-courses measured by SALS transmission intensity are given for PDS and the PDS-copolymer at 70 °C. This low-shear rate was chosen so as to enhance the crystallization kinetics, without disturbing the developing morphology. These step-shear

Table 1
Avrami parameters for the crystallization kinetics of PDS and the PDS-copolymer at selected crystallization temperatures and shear conditions. The step-shear was applied for 1 s at a shear rate of 60 s^{-1}

	Quiescent			Step-shear		
T_c (°C)	n	k	$t_{1/2}$ (s)	n	k	$t_{1/2}$ (s)
PDS						
60	2.6	5.10×10^{-8}	480	2.2	2.50×10^{-6}	300
65	2.3	1.80×10^{-7}	720	2.1	3.40×10^{-6}	350
70	2.5	9.00×10^{-9}	1260	1.8	1.30×10^{-5}	390
75	2.6	7.30×10^{-10}	2230	1.7	9.70×10^{-6}	670
80	n/a	n/a	>9000	1.8	8.50×10^{-6}	540
85	n/a	n/a	n/a	1.8	3.10×10^{-6}	1140
90	No crystallization	No crystallization	No crystallization	1.8	1.00×10^{-6}	1860
PDS-copolymer						
70	3	9.90×10^{-13}	8220	2	3.10×10^{-7}	1500

n/a: Data from SAXS, Avrami parameters not determined.

crystallization data are best summarized by considering the $t_{1/2}$ behavior over a wide range of crystallization temperatures, as shown in Fig. 5. It is noteworthy that the shear-enhancement to kinetics is temperature-dependent, increasing with crystallization temperature.

To further understand this observation, at this point we compare nucleation and growth rates from optical microscopy for selected crystallization runs under crystallization conditions where these values are most easily determined. For example, in the case of PDS crystallization at 75 °C, the quiescent growth rate was found to be 3.8 μm/min, while for the same thermal conditions but with a 60 s^{-1} step-shear the growth rate was 4.2 μm/min. The difference is not considered significant. The nucleation densities when compared at 3 min, the earliest time in the crystallization when distinct patterns emerge in the microscope, were found to be 37×10^3 cm^{-3}, while for the step-sheared sample there were approximately 6.1×10^6 cm^{-3}. In the case of PDS crystallization at 80 °C the quiescent nucleation density at 5 min was 15×10^3 cm^{-3}, while the step-sheared sample contained approximately 6×10^6 cm^{-3}. Shear-induced increases in nucleation density have been noted previously. In a steady-shear experiment on poly(1-butene) (95 °C, shear rate of 3 s^{-1}), Wolkowicz [8] found an approximately 750 fold increase in nucleation density and Floudas et al. [23] found a 30 fold increase in nucleation density in their steady-shear experiment on the polyester poly(ϵ-caprolactone), performed at 55 °C under 500 Pa stress.

Due to experimental difficulties in quenching the melt rapidly enough, it was not possible to perform reliable experiments at lower crystallization temperatures. However, the merging of the $t_{1/2}$ values from shear-induced and quiescent processes strongly suggests that there is a limit to the ability of nucleation-enhancing shear to produce nuclei,

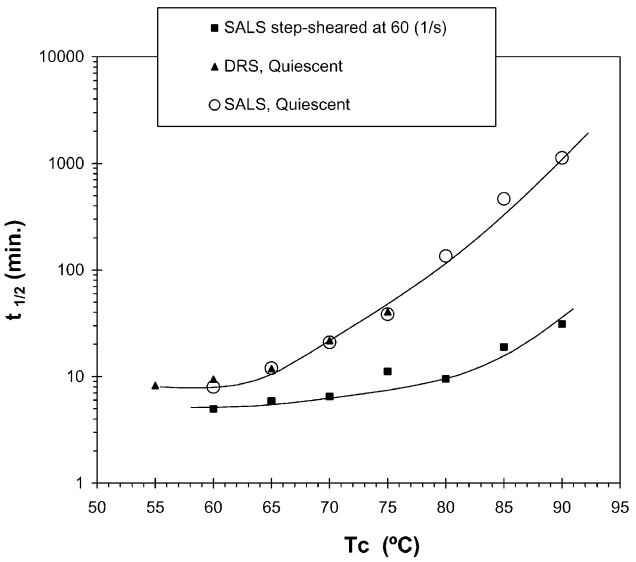

Fig. 5. Crystallization half-time by SALS transmission vs. crystallization temperature comparison of quiescent and step-shear (60 s^{-1}) kinetics for PDS. Selected quiescent half-time data by DRS are shown. The solid curves are guides for the eye.

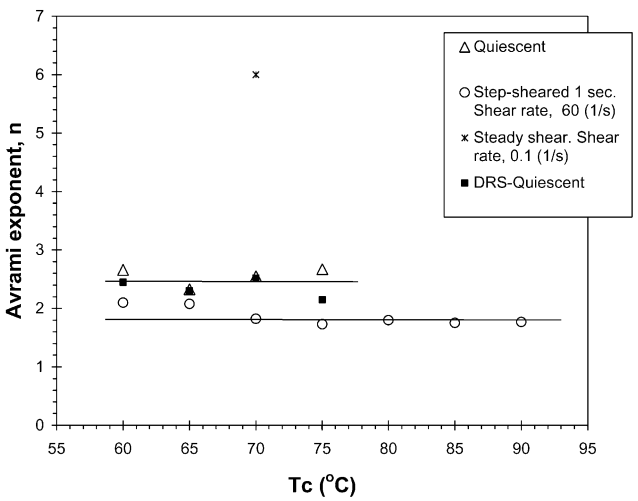

Fig. 6. Avrami exponent, n, vs. crystallization temperature comparison of quiescent, step-shear (60 s^{-1}), and steady-shear (0.1 s^{-1}) kinetics for PDS. Selected quiescent data by DRS are shown.

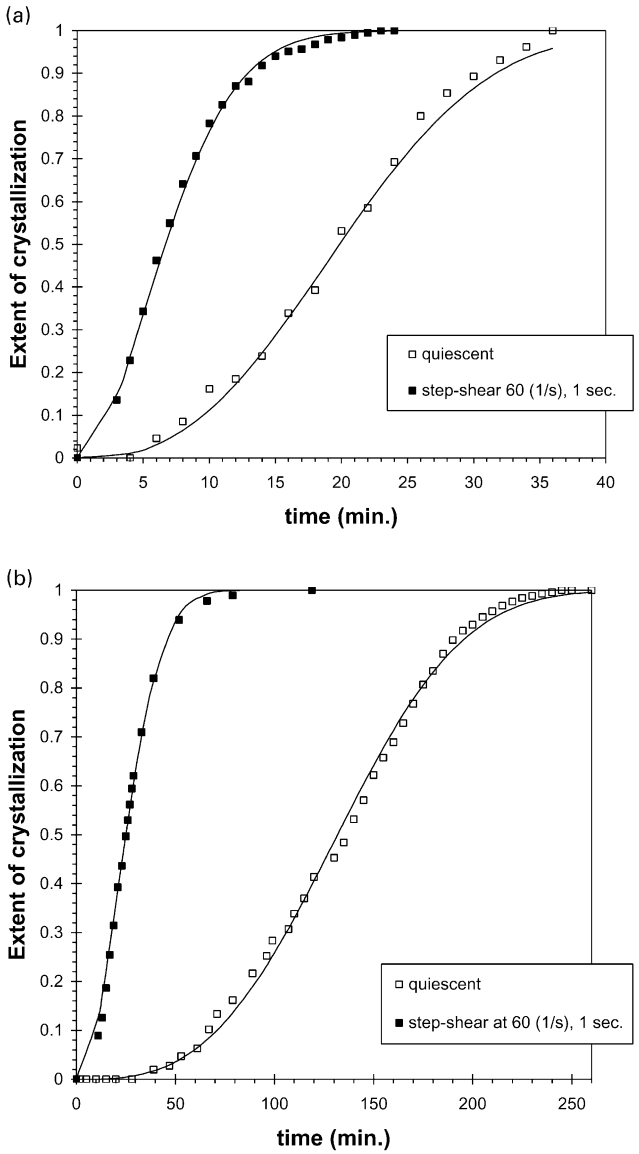

Fig. 7. Extent of crystallization time-course measured by SALS transmission at: (a) 75 °C for PDS under quiescent and step-shear 60 s^{-1} conditions, and (b) 70 °C for the PDS-copolymer under quiescent and step-shear 60 s^{-1} conditions.

and at sufficiently low temperatures (for PDS, below 55 °C) the step-shear-induced nuclei do not exceed the thermal nuclei present at this temperature.

In addition to the enhancement in crystallization kinetics over quiescent kinetics, the application of a step-shear also results in a systematic drop in the Avrami *n* exponent. This comparison between quiescent and step-shear crystallization Avrami *n* values is shown over a wide range of crystallization temperatures in Fig. 6. As mentioned earlier, the figure also reveals a generally good agreement of the Avrami exponent between variety of experimental techniques (calorimetry [19], SAXS [25], and DRS [15]) probing rather different aspects of the crystallization process. The *decrease* in *n* with step-shear over quiescent *n* is unexpected, considering previous work under steady-

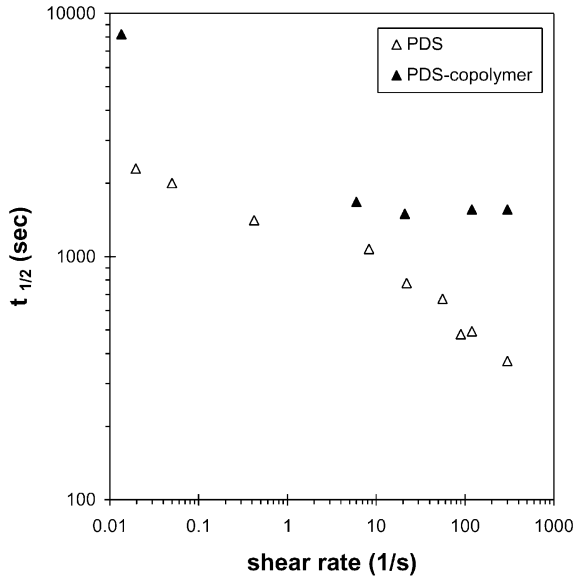

Fig. 8. Crystallization half-time by SALS transmission vs. step-shear rate (shear duration of 1 s) for PDS at 75 °C and the PDS-copolymer at 70 °C.

shear conditions. The work of Sherwood et al. [7] on polymers crystallized under steady-shear conditions showed that *n increases* systematically with increasing shear rate. Fig. 6 also shows that *n* does not depend on temperature for sheared or quiescently crystallized polymers. A study by Tribout et al. [9] on step-shear-induced crystallization of a polypropylene copolymer utilized a two-step Avrami model to analyze the crystallization kinetics. They found an unusually high Avrami *n* for the initial portion of the kinetics. In the present work, we feel that a single Avrami term fits the data well (cf. Figs. 4 and 7a,b), and the addition of a second term is unneeded, and would unnecessarily complicate the interpretation of the best-fit Avrami parameters. We do not wish to over-interpret the trend in the Avrami exponent between sheared and unsheared polymers, but we can note that the systematic drop in the exponent agrees with the microscopy observations of a shear-dependent change in nucleation.

The crystallization-enhancing influence of a step-shear increases over the range of shear rates examined. This is seen in Fig. 8 by the decrease in $t_{1/2}$ as a function of shear rate. These data were collected under experimentally convenient conditions—75 °C for PDS and 70 °C for the PDS-copolymer. We must note that in our experiments, when we increase the shear rate, the over-all strain increases from a value of 1000% for a shear rate of 10 s^{-1} to a value of 30,000% for a shear rate of 300 s^{-1}, this is due to a minimum shear time in our shear cell of 1 s. Although a large range of strains and shear rates were explored, the crystallization process was nucleation-enhancing for all of the step-shear runs on both polymers—random spherulitic growth was found.

Since the application of step-shear was found to induce

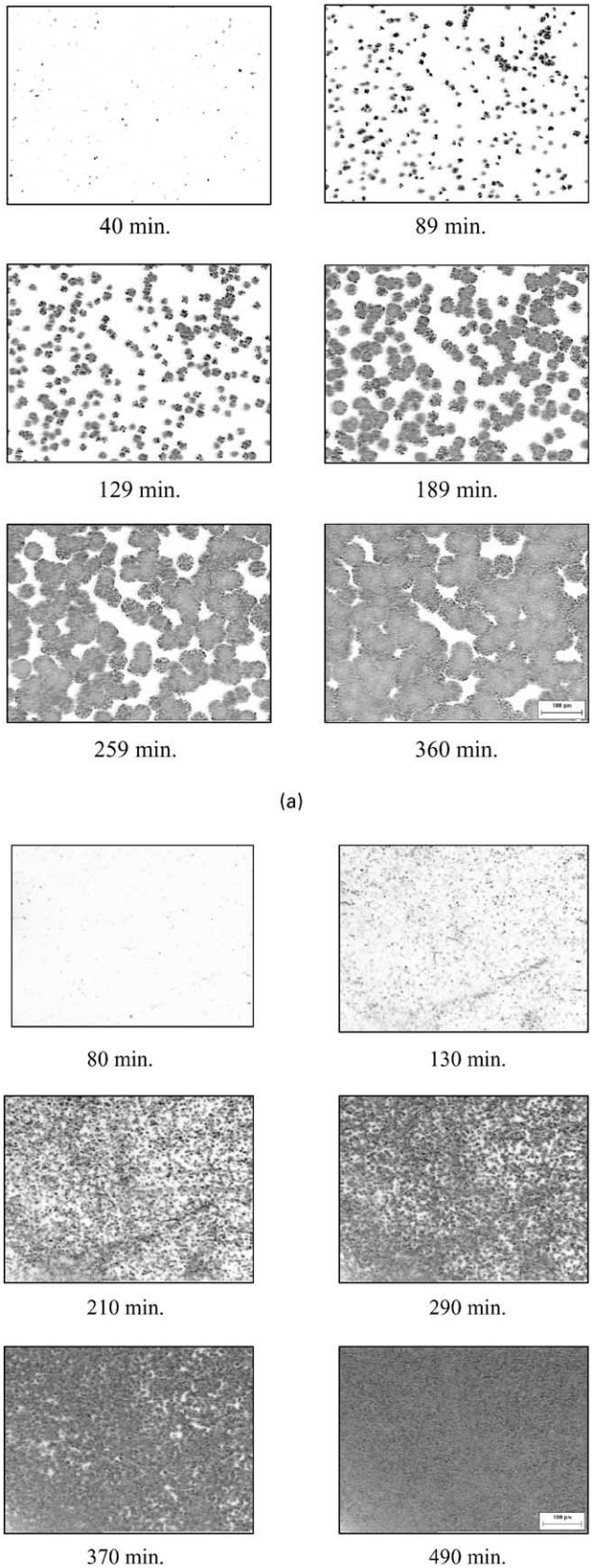

nuclei in the polymers under study, it was of interest to explore the ability to do so at temperatures where no quiescent crystallization was observed. Two experiments were performed under isothermal conditions where no quiescent crystallization had occurred for very long time (for both polymers no indications of crystallization were observed to 72 h) at 95 °C for PDS, and for the PDS-copolymer at 90 °C. The step-shear experimental procedure was the same as used previously—an isothermal hold at 140 °C for 5 min to melt the polymer, a lowering of the shear cell windows to create the 140 μm film thickness, and an additional 5 min at 140 °C to remove stress. Then the temperature was reduced at 30 °C/min to the crystallization temperature. Once the sample reached the crystallization temperature, a 1 s step-shear (60 s^{-1}) was applied. For both polymers this step-shear application was sufficient to induce the crystallization process, as shown via optical micrographs in Fig. 9a for PDS and Fig. 9b for the PDS-copolymer. For PDS the nucleation density was 1.3×10^6 cm^{-3} (at 90 min) and the growth rate was 0.2 μm/min, and for the PDS-copolymer the initial nucleation density was an order of magnitude higher $\sim 12.3 \times 10^6$ cm^{-3} (at 90 min). We were not able to determine the growth rate for the copolymer under these conditions, as the spherulite size was very small when impingement occurred. Crystallization at these temperatures provides for an examination of shear-induced nuclei, since thermal nuclei do not form. The process appears to be one of a rapid activation of the nuclei during the step-shear, followed only by growth for the remainder of the crystallization. This is supported by the uniformity of object sizes in the image, and in particular, at later times, no small objects (new nuclei) appear. A phenomenon is occurring during these high temperature crystallization processes that may at first appear to be thermal, homogeneous nucleation, but has a different origin. We discuss this phenomenon later.

In Fig. 9a and b the increasing number of objects that appear with time is due to the developing orientation in the spherulites—some of the objects at early times do not have sufficient lamellae oriented at ~45° to the polarizers to allow any depolarized light to pass. However, at later times, in the same object these lamellae form, which results in a large object suddenly appearing in the image (cf. compare the images taken at 40 min to those taken at 80 min). If these were thermal nuclei forming at these temperatures, at long times, e.g. 189 min in Fig. 9a, objects of smaller size would be present among the larger developing spherulites.

Fig. 9. Optical micrographs taken at selected times during the isothermal crystallization after a 1 s step-shear (60 s^{-1}) of: (a) PDS at 95 °C, and (b) PDS-copolymer at 90 °C.

4. Conclusions

It has been shown that the crystallization kinetics of both PDS and the PDS-copolymer can be greatly enhanced by the application of a step-shear. The enhancement is via an increase in nucleation density. The nucleation-enhancing step-shear serves to activate a large number of nuclei, which subsequently grow in the same manner and morphology as in the quiescent case. The number of nuclei formed during the relatively short shearing time is large compared to the number which are formed during the quiescent phase. One consequence of nucleation-enhancing shear is uniformity in spherulite size.

The crystallization kinetics enhancement from a step-shear decreases with decreasing crystallization temperature. This may be unexpected, but can be explained by the following. With decreasing temperature and thus increasing polymer viscosity the ability to orient chains by shear and for those induced orientations to persist and not relax will increase. This would lead to an expectation of increasing shear-induced nucleation densities with decreasing temperature, hence, a greater shear-enhancement on crystallization kinetics with decreasing temperature. Two competing factors frustrate this prediction. The first is that the quiescent nucleation density increases with decreasing temperature (increasing degree of undercooling). The second is that there are a finite number of nuclei that can be activated by a given step-shear. This is suggested by the power-law trend in crystallization half-time with increasing shear rate at constant crystallization temperature in Fig. 8. This trend indicates an increasing number of activated nuclei with shear rate. These two factors taken together result in the fact that at the lower crystallization temperatures, the step-shear-induced nuclei (at $60\,s^{-1}$) do not significantly exceed the thermal nuclei (present in the quiescent case), and since spherulite growth rates are found to be unchanged by step-shear, the over-all crystallization kinetics are not greatly enhanced by shear at these lower temperatures.

In addition to these findings, three others may be enumerated: (1) the spherulite growth rates of the polymers under study were unaffected by the application of a step-shear, (2) this step-shear is in the nucleation-enhancing shear regime for the polymers investigated; spherulites develop and are distributed randomly throughout the samples, and (3) the steady-shear conditions applied to the polymers result in a deforming crystallization process; deformed spherulites, and ultimately fibrillar morphologies are observed.

Finally, we may comment on the following questions raised by the present work: why is nucleation-enhancing shear possible? Why do the nuclei induced by shear not result in fibrillar morphologies? Several explanations present themselves. The first is that the molecular orientation induced by shear was insufficient. For a given molecular weight distribution, there is a critical molecular extension required to produce fibrillar morphologies [13]. Molecular extensions by shear that are below this threshold, due to insufficient strain or to molecular relaxation occurring following a shear step, will result in chains that register in segments of sufficient length to create stable nuclei, but not long enough to nucleate extended-chain microfibrils or other oriented structures. We have shown that larger strains from steady-shear allows more time for both longer chain segments to register, forming fibrils, and for the deformation of mature spherulites.

Acknowledgments

This work was supported by a Johnson & Johnson Corporate Office of Science and Technology (COSAT) Excellence in Science Award Grant. The authors would like to thank Nitash Balsara (University of California, Berkley), Bruce Garetz (Polytechnic University, Brooklyn, NY), and Jerry Fischer (Ethicon, Somerville, NJ) for helpful discussions regarding the SALS experimental set-up. The authors would also like to thank Ed Dormier (Ethicon, Somerville, NJ) for helpful comments and support.

References

[1] Eder G, Janeschitz-Kriegl H, Liedauer S. Prog Polym Sci 1990;15:629.
[2] Ulrich R, Price F. J Appl Polym Sci 1976;20:1095.
[3] Pogodina N, Lavrenko V, Srinivas S, Winter H. Polymer 2001;42:9031.
[4] Kumaraswamy G, Issaian A, Kornfield J. Macromolecules 1999;32:7537.
[5] Matsushige K, Nagata K, Imada S, Takemura T. Polymer 1980;21:1391.
[6] Wang Y, Cakmak M, White J. J Appl Polym Sci 1985;30:2615.
[7] Sherwood C, Price FP, Stein RS. J Polym Sci, Polym Symp 1978;63:77.
[8] Wolkowicz M. J Polym Sci, Polym Symp 1978;63:365.
[9] Tribout C, Monasse B, Haudin JM. Colloid Polym Sci 1996;274:197.
[10] Flory PJ. J Chem Phys 1947;15:397.
[11] Magill J. Rates of crystallization of polymers. In: Brandrup J, Immergut E, Grulke E, editors. Polymer handbook, 4th ed. New York: Wiley; 1999. p. 280. Chapter VI.
[12] Keller A, Kolnaar H. Flow induced orientation and structure formation. In: Meijer H, editor. Processing of Polymers, vol. 18, 1997. p. 189.
[13] Somani R, Hsiao B, Nogales A, Srinivas S, Tsou A, Sics I, Balta-Calleja F, Ezquerra T. Macromolecules 2000;33:9385.
[14] Nogales A, Hsiao B, Somani R, Srinivas S, Tsou A, Balta-Calleja F, Ezquerra T. Polymer 2001;42:5247.
[15] Andjelić S, Fitz B. J Polym Sci, Part B: Polym Phys 2000;38:2436.
[16] Andjelić S, Jamiolkowski DD, McDivitt J, Fischer J, Zhou J. J Polym Sci, Polym Phys Ed 2001;39:3073.
[17] Doddi N, Vesfelt C, Wasserman D. (Ethicon, Inc.) synthetic absorbable surgical devices of poly(*p*-dioxanone). US Patent 4,052,988; 1977.
[18] Bezwada R, Jamiolkowski D, Cooper K. In: Domb AJ, Kost J, Wiseman DM, editors. Handbook of biodegradable polymers. Singapore: Harwood Academic; 1997. p. 29–61. Chapter 2.

[19] Andjelić S, Jamiolkowski D, McDivitt J, Fischer J, Zhou J, Vetrecin R. J Appl Polym Sci 2001;79:742.
[20] Dai HJ. PhD Dissertation, New York: Polytechnic University; June 1998.
[21] Pogodina N, Siddiquee S, van Egmond JW, Winter H. Macromolecules 1999;32:1167.
[22] Stein R, Rhodes M. J Appl Phys 1960;31:1873.
[23] Floudas G, Hilliou L, Lellinger D, Alig I. Macromolecules 2000;33:6466.
[24] Avrami M. J Chem Phys 1939;7:1103.
[25] Andjelić S, Jamiolkowski D, McDivitt J, Fischer J, Zhou J, Wang Z, Hsiao B. J Polym Sci, Part B: Polym Phys 2001;39:153.